Mineralogical Magazine, October 2016, Vol. 80(6), pp. 1077–1088

Tvrdýite, $Fe^{2+}Fe^{3+}_2Al_3(PO_4)_4(OH)_5(OH_2)_4{\cdot}2H_2O$, a new phosphate mineral from Krásno near Horní Slavkov, Czech Republic

J. Sejkora[1,*], I. E. Grey[2], A. R. Kampf[3], J. R. Price[4] and J. Čejka[1]

[1] Department of Mineralogy and Petrology, National Museum, Cirkusová 1740, Praha 9, 193 00, Czech Republic
[2] CSIRO Mineral Resources, Private Bag 10, Clayton South, Victoria 3169, Australia
[3] Mineral Sciences Department, Natural History Museum of Los Angeles County, 900 Exposition Boulevard, Los Angeles, CA 90007, USA
[4] Australian Synchrotron, 800 Blackburn Road, Clayton, Victoria 3168, Australia

[*Received 30 June 2015; Accepted 22 October 2015; Associate Editor: Juraj Majzlan*]

ABSTRACT

Tvrdýite, $Fe^{2+}Fe^{3+}_2Al_3(PO_4)_4(OH)_5(OH_2)_4{\cdot}2H_2O$, is a new phosphate mineral from the abandoned Huber open pit, in the Krásno ore district near Horní Slavkov, western Bohemia, Czech Republic. It was found along with Al-rich beraunite, fluorapatite and pharmacosiderite in a cavity of quartz gangue. Tvrdýite forms acicular to fibrous crystals with diameters in the range 0.5–5 μm and lengths up to 300 μm, partly grouped in radiating aggregates up to 3 mm in size. It has a silvery to olive, greyish green colour with pearly lustre, greyish-white streak and is very brittle with an uneven fracture; individual fibres are somewhat flexible. Cleavage on {100} is good; the Mohs hardness is ~3–4. The calculated density is 2.834 g cm^{-3}. Tvrdýite is optically biaxial (–), with $\alpha = 1.650(2)$, $\beta = 1.671(1)$ and $\gamma = 1.677(1)$ (white light); $2V = 56(1)°$; dispersion: $r > v$, strong; optical orientation: $Z = b$, $X \approx a$, $Y \approx c$; pleochroism: X = greenish blue, Y = yellowish orange, Z = yellowish orange ($X >> Y > Z$). Tvrdýite is monoclinic, space group $C2/c$, $a = 20.564(4)$, $b = 5.101(1)$, $c = 18.883(4)$ Å, $\beta = 93.68(3)°$ and $V = 1976.7(7)$ Å^3, $Z = 4$, $a:b:c = 4.031:1:3.702$. The strongest eight lines in the powder X-ray diffraction (XRD) pattern [d in Å (I)(hkl)] are 10.227 (100) (200), 9.400 (6) (002), 7.156 (14) ($20\bar{2}$), 5.120 (7) (400), 3.416 (11) (600), 3.278 (6) ($60\bar{2}$), 2.562 (5) (800) and 2.0511 (3) ($\bar{1}0$,0,0). Chemical analyses by electron microprobe yielded MnO 0.01, ZnO 5.08, FeO 4.31, Fe_2O_3 21.16, Al_2O_3 16.71, P_2O_5 32.64, As_2O_5 2.56, F 0.53, H_2O (calc.) 17.84, O = F –0.22, total 100.62 wt.%. The resulting empirical formula, calculated on the base of 27 anions, obtained from the crystal structure, is $Zn_{0.52}Fe^{2+}_{0.50}Fe^{3+}_{2.21}Al_{2.75}(PO_4)_{3.86}(AsO_4)_{0.19}OH_{4.60}F_{0.23}(OH_2)_4{\cdot}2H_2O$. The ideal formula, $Fe^{2+}Fe^{3+}_2Al_3(PO_4)_4(OH)_5(OH_2)_4{\cdot}2H_2O$, requires FeO 8.75, Fe_2O_3 19.44, Al_2O_3 18.62, P_2O_5 34.56, H_2O 18.64, total 100.00 wt.%. The crystal structure of tvrdýite was solved from single-crystal data (synchrotron beamline) and refined to $R_1 = 0.038$ for 2276 reflections with $I > 2\sigma(I)$. Tvrdýite is isostructural with beraunite, but contains dominant Al in two of the four independent M sites, which are all occupied by Fe in beraunite.

Keywords: tvrdýite, new mineral, phosphate, beraunite, crystal structure, Krásno near Horní Slavkov, Czech Republic.

Introduction

The mineral beraunite, ideally $Fe^{2+}Fe^{3+}_5(PO_4)_4(OH)_5(OH_2)_4{\cdot}2H_2O$, was described for the first time from the Hrbek mine at Svatá Dobrotivá (St Benigna) near Beroun (Beraun), central Bohemia, Czech Republic, by Breithaupt (1841). More recently, beraunite was studied by Fanfani and Zanazzi (1967), Marzoni Fecia di Cossato *et al*. (1989) and Moore and Kampf (1992). It is known from many localities worldwide (Anthony *et al.*, 2000).

*E-mail: jiri_sejkora@nm.cz
DOI: 10.1180/minmag.2016.080.045

During our investigations of late hydrothermal and supergene F-rich phosphate assemblages from Krásno ore district a number of rare and unusual minerals have been discovered. One of this suite was an interesting 'beraunite' with significant contents of Al and Zn (Sejkora *et al.,* 2006*c*), which have not been previously described for this mineral phase. In this paper, we report the description of a new mineral, tvrdýite, found at Krásno. The new mineral is an analogue of beraunite in which Al^{3+} replaces Fe^{3+} as the dominant cation in two of the four Fe sites in the beraunite structure, providing the ideal formula $Fe^{2+}Fe^{3+}_2Al_3(PO_4)_4(OH)_5(OH_2)_4 \cdot 2H_2O$. The new mineral honours the Czech mineralogist and geologist Dr Jaromír Tvrdý (b. 1959) from Liberec, northern Bohemia, Czech Republic, for his contributions to mineralogy and economic geology. Dr Tvrdý is the author of papers on the mineralogy and geology of the Krásno – Horní Slavkov area (e.g. Plášil and Tvrdý, 2008; Sejkora and Tvrdý, 2009) and surrounding occurrences (Sejkora *et al*., 2008; Tvrdý and Plášil, 2010; Pažout *et al*., 2015). The pronunciation of tvrdýite is /twe:(r) 'di: ait/, or using special characters /twɜːʳ ˈdiː aɪt/. This would be similar to 'twerdeeite'.

The new mineral and name have been approved by the Commission on New Minerals, Nomenclature and Classification of the International Mineralogical Association (IMA 2014-082). The holotype specimen (one sample 5 cm × 4 cm × 2 cm) is deposited in the collections of the Department of Mineralogy and Petrology of the National Museum in Prague, Cirkusová 1740, Praha 9, Czech Republic, catalogue number P1P 11/2014. Parts of the holotype are also deposited at Museum Victoria, Melbourne, Australia, specimen number M53361 and in the Natural History Museum of Los Angeles County, Los Angeles, USA, catalogue number 65560.

Occurrence

The Krásno ore district near the Horní Slavkov, Slavkovský les area (Czech Republic) is one of the most important areas of tin and tungsten mining in central Europe (Beran and Sejkora, 2006). The district is characterized by greisen mineralization in several granite cupolas of the large Krušné hory (Erzgebirge) granite batholith underlying metamorphic rock (mainly gneisses). The largest Sn-W deposit in this district is the Huber stock; in the past, it was mined from the Huber open pit and Huber (Stannum) shaft up to 200 m under the surface. The stock is bell-shaped in section, similar to a blunt cone. At 100 m under the present surface, the size is 200 m × 100 m, at 150 m under the surface, the stock extends 400 m NE-SW and is ~250 m wide. The Huber stock consists basically of autometamorphosed Li-mica-topaz granite with a variable degree of greisenization. It is assumed that the whole apical part of this cupola was formed by greisen and quartz with rich ore mineralization (Beran and Sejkora, 2006). Detailed descriptions of the mineralogy (more than 230 mineral species) of the Krásno ore district were published by Beran and Sejkora (2006) and Sejkora *et al*. (2006*a*–*c*). More recently, the new minerals krásnoite (Mills *et al*., 2012) and iangreyite (Mills *et al*., 2011) were described from this locality, which also hosts the second world occurrence of kunatite (Mills *et al*., 2008) and plimerite (Sejkora *et al*., 2011).

Tvrdýite was found in late hydrothermally and supergene altered phosphate accumulations in the abandoned Huber open pit in the Krásno ore district (50°07'22"N 12°48'2"E). The pit exposes the top part of Huber stock; it is completely greisened and contains quartz bodies with disseminated cassiterite, wolframite, sulfides and phosphates and, in the past, was mined for Sn and W (Sejkora *et al*., 2006*c*). Tvrdýite was found in a cavity in quartz gangue in association with older, greenish brown, Al-rich (1–1.5 atoms per formula unit (apfu) Al) beraunite, white fluorapatite and yellowish green pharmacosiderite. It is a late hydrothermal or supergene mineral formed from the breakdown of primary triplite (in association with isokite and fluorapatite) in contact with acidic waters.

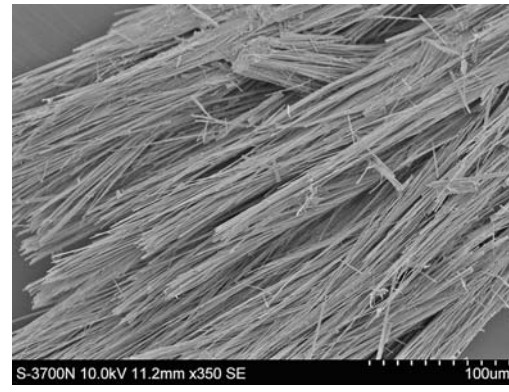

FIG. 1. Photomicrograph of multiply intergrown fibrous crystals of tvrdýite from Krásno. Secondary electron image (Hitachi 3700N).

Physical and optical properties

Tvrdýite occurs as thin lath crystals elongated on [010] and flattened on {100} with diameters in the range 0.5–5 μm and lengths up to 300 μm (Fig. 1), commonly grouped in radiating aggregates up to 3 mm in size (Fig. 2). Aggregates are silvery to olive greyish green with a pearly lustre. Tvrdýite aggregates are opaque, but individual fibrous crystals are translucent to transparent. It has a light olive-green streak. Aggregates are very brittle, but individual fibres are somewhat flexible. The Mohs hardness is estimated to be 3–4 by analogy with beraunite and the mineral has a good cleavage on {100}. A density of 2.834 g cm^{-3} was calculated using the empirical formula and unit-cell parameters obtained from single-crystal XRD data. Density measurements were not undertaken due to paucity of the pure material and its fibrous nature. Tvrdýite is non-fluorescent under shortwave or longwave ultraviolet radiation. It is optically biaxial (–), with indices of refraction measured using white light $\alpha = 1.650(2)$, $\beta = 1.671(1)$, $\gamma = 1.677(1)$. The measured 2V is 56(1)° based on extinction data using *EXCALIBR* (Gunter *et al*., 2004) and is identical to the calculated value. Observed dispersion is strong with $r > v$. Optical orientation is $Z = b$, $X \approx a$, $Y \approx c$. Tvrdýite is pleochroic with X = greenish blue, Y = yellowish orange, Z = yellowish orange ($X >> Y > Z$). The Gladstone-Dale compatibility index $1 - (K_P/K_C)$ is 0.022 for the empirical formula and unit-cell parameters from single-crystal XRD data, indicating excellent compatibility (Mandarino, 1981).

FIG. 2. Olive-grey to green fibrous aggregates of tvrdýite from Krásno. Field of view is 5 mm; photo by Jiří Sejkora.

Chemical composition

The chemical composition of tvrdýite (Table 1) was determined using a Cameca SX100 electron microprobe (wavelength-dispersive spectroscopy mode, 15 kV, 10 nA, 8 μm beam diameter) from nine analytical points. The following X-ray lines and standards were selected; $L\alpha$ line: As (lammerite); $K\alpha$ lines: P, Ca (fluorapatite), Al, K (sanidine), Zn (gahnite), Fe (almandine), Mg (syn. Mg_2SiO_4), Na (albite), Si, Mn (spessartine), Ti (titanite), Cl (vanadinite) and F (topaz). Contents of Na, K, Ca, Mg, Ti, Si and Cl were below detection limits (~0.05 wt.%). Peak counting times (CT) were 10–20 s and the counting time for background was 50% of the peak CT. The measured intensities were processed for matrix effects using the '*PAP*' correction routine (Pouchou and Pichoir, 1985). Water could not be analysed directly because of the minute amount of material available; it was calculated on the basis of 17 H apfu, from the structure analysis, corrected for partial substitution of F for OH.

The significant contents (in apfu) of Fe (2.61–2.83), Al (2.55–2.80), Zn (0.46–0.56) and P (3.75–3.85) are characteristic for the holotype sample of tvrdýite. Results of electron probe microanalyses (EPMA) show strong negative Al-Fe correlation (Fig. 3); contents of Zn do not correlate with Fe or Al. A strong positive correlation was observed for Al-F (Fig. 4). This suggests that Al replacement for Fe in beraunite resulted from a reaction with F-rich acidic solutions; however, the maximum amount of F in tvrdýite is only 0.25 apfu. A small content of As (0.16–0.22 apfu) was found in the tetrahedral sites, but there is only a weak correlation between As and P (Fig. 5). The empirical formula of tvrdýite (based on 27 anions pfu) is $Zn_{0.52}Fe^{2+}_{0.50}Fe^{3+}_{2.21}Al_{2.75}(PO_4)_{3.86}(AsO_4)_{0.19}(OH)_{4.60}F_{0.23}(OH_2)_4 \cdot 2H_2O$. Based on the structure analysis (see below), Zn is not dominant at any specific site; at $M1$ $Fe^{2+} >> Fe^{3+}$, Zn; at $M2$ $Al >> Fe^{3+}$; at $M3$ $Al > Fe^{3+}$,Zn and at $M4$ $Fe^{3+} >$Al,Zn. The simplified formula ($M1$–$M4_2$–$M2$–$M3_2$) is thus $(Fe^{2+},Fe^{3+},Zn)(Fe^{3+},Al,Zn)_2(Al,Fe^{3+})(Al,Fe^{3+})_2(PO_4)_4(OH)_5(OH_2)_4 \cdot 2H_2O$. The ideal formula is $Fe^{2+}Fe^{3+}_2Al_3(PO_4)_4(OH)_5(OH_2)_4 \cdot 2H_2O$, which requires FeO 8.75, Fe_2O_3 19.44, Al_2O_3 18.62, P_2O_5 34.56, H_2O 18.64, total 100.00 wt.%.

Vibrational spectroscopy

The ideal formula of monoclinic tvrdýite, space group $C2/c$, $Z = 4$, is $Fe^{2+}Fe^{3+}_2Al_3(PO_4)_4(OH)_5$

TABLE 1. Chemical composition of tvrdýite in comparison with associated Al-rich beraunite.

	Tvrdýite			Al-rich beraunite		
	Mean (n = 9)	Range	SD	Mean (n = 7)	Range	SD
MnO	0.01	0–0.06	0.02	0.02	0–0.09	0.04
ZnO	5.08	4.56–5.45	0.30	6.01	5.29–6.44	0.42
FeO*	4.31*			4.14		
Fe_2O_3*	21.16*			31.70		
Al_2O_3	16.71	15.6–17.3	0.53	7.54	6.59–8.68	0.77
P_2O_5	32.64	32.1–33.0	0.25	31.39	30.1–31.9	0.64
As_2O_5	2.56	2.19–3.01	0.32	2.19	1.78–3.88	0.75
F	0.53	0.45–0.58	0.04	0.17	0.12–0.24	0.04
H_2O**	17.84			17.16		
O = F	–0.22			–0.07		
Total	100.62			100.25		
Calculation based on 27 anions pfu obtained from the crystal structure						
Mn	0.00			0.00		
Zn	0.52			0.65		
Fe^{2+}	0.50			0.50		
Fe^{3+}	2.21			3.50		
Al	2.75			1.31		
P	3.86			3.90		
As	0.19			0.17		
F	0.23			0.08		
OH	4.60			4.81		
H_2O	6.00			6.00		

*Calculated from total Fe as FeO of 23.35 wt.%, range 22.75–24.42, SD [standard deviation] = 0.54 (tvrdýite) and mean 32.66 wt.%, range 31.74–33.59, SD = 0.73 (Al-rich beraunite), on the basis of 0.5 Fe^{2+} pfu, from bond-valence calculations. **Water was calculated on the basis of 17 H apfu, from the structure analysis, corrected for partial substitution of F for OH.

$(OH_2)_4 \cdot 2H_2O$. The crystal structure of tvrdýite contains two symmetrically distinct phosphate groups, five symmetrically distinct hydroxyls and two symmetrically distinct water molecules. The free $(PO_4)^{3-}$ ion, possessing T_d point symmetry, is characterized by four fundamentals, the ν_1 (A_1)

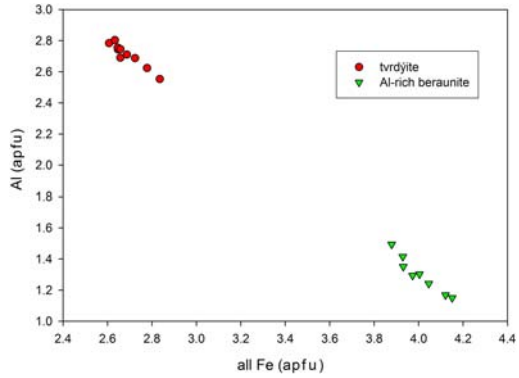

FIG. 3. The contents Fe *vs.* Al (apfu) for tvrdýite and associated Al-rich beraunite.

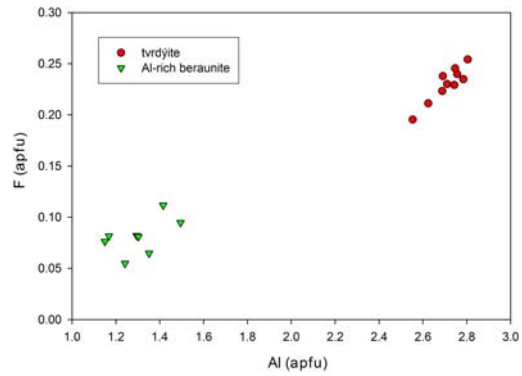

FIG. 4. The contents Al *vs.* F (apfu) for tvrdýite and associated Al-rich beraunite.

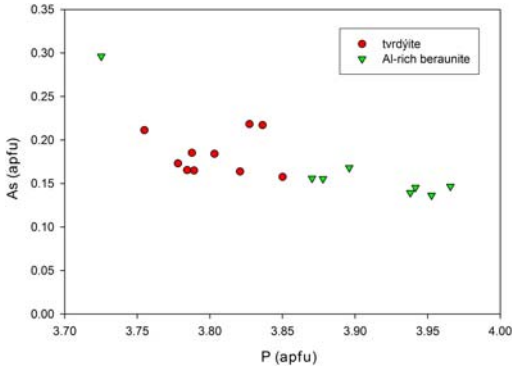

FIG. 5. The contents P *vs.* As (apfu) for tvrdýite and associated Al-rich beraunite.

symmetric stretching vibration, the ν_2 (δ) (*E*) doubly degenerate bending vibration, the ν_3 (F_2) triply degenerate antisymmetric stretching vibration, and the ν_4 (δ) (F_2) triply degenerate bending vibration. Corresponding band wavenumbers are located approximately in the range 410–490 (ν_2), 510–670 (ν_4), 930–990 (ν_1) and 975–1140 (ν_3) cm^{-1}, respectively (Pechkovskii *et al.,* 1981). All vibrations are Raman active; the ν_3 and ν_4 vibrations are also infrared active. Any symmetry lowering may cause infrared activation of all vibrations and splitting of degenerate vibrations (Nakamoto, 1986). Molecular water, point symmetry C_{2v} is characterized by three fundamentals, the symmetric stretching vibration ν_1 (A_1) OH, and the antisymmetric stretching vibration ν_3 (B_1) OH, both in the range of ~3600–2900 cm^{-1}, and the bending vibration ν_2 (A_1) H_2O (δ H_2O) in the range of ~1700–1590 cm^{-1} and libration modes in the range ~900–300 cm^{-1} (Nakamoto, 1986). All vibrations are Raman and infrared active; however, there are sometimes problems in the recording and resolution of the Raman bands. Hydroxyl ions, OH^-, (point symmetry $C_{\infty v}$) are indicated commonly by sharp bands between 3700 and 3450 cm^{-1}, but sometimes at lower wavenumbers, if any appreciable amount of hydrogen bonding is involved, δ M–OH at ~1500 cm^{-1} and over a wide range below this value, and OH libration modes in the spectra range from 1000 to 300 cm^{-1} (Lutz, 1995).

The infrared vibrational spectrum of tvrdýite was recorded by the attenuated total reflection method on a Nicolet iS50 spectrometer (range 4000–400 cm^{-1}, resolution 4 cm^{-1}, 64 scans). The main bands (Fig. 6) observed are (cm^{-1}) at 3610, 3394, 3255, 1631, 1191, 1058, 1017, 994, 936, 843, 613 and 485. A band at 3610 cm^{-1} is assigned to the ν OH stretching vibrations of hydroxyl ions. Bands at 3394 and 3255 cm^{-1} are attributed to the ν OH stretching vibrations of symmetrically distinct hydrogen-bonded water molecules. O–H···O hydrogen bond lengths vary in the range from approximately >3.2 to 2.73 Å (Libowitzky, 1999). A band at 1631 cm^{-1} is assigned to the ν_2 (δ)

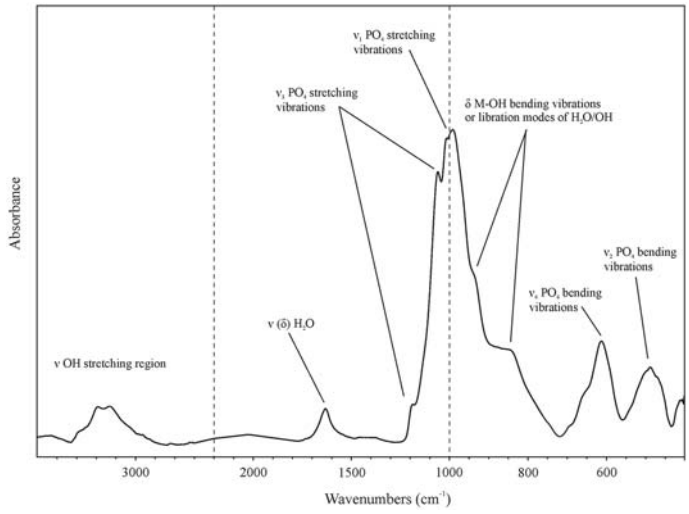

FIG. 6. The infrared spectrum of tvrdýite; the *x* axis was rescaled at 2200 and 1000 cm^{-1} to emphasize selected features in the spectrum.

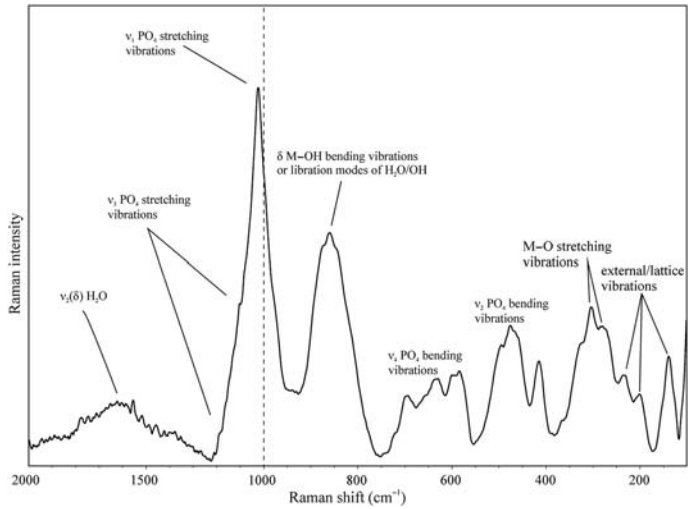

FIG. 7. The Raman spectrum of tvrdýite; the *x* axis was rescaled at 1000 cm^{-1} to emphasize selected features in the spectrum.

bending vibrations of water molecules. Bands at 1191 and 1058 cm^{-1} are assigned to the ν_3 $(PO_4)^{3-}$ antisymmetric stretching vibrations, and those at 1017 and 994 cm^{-1} to the ν_1 $(PO_4)^{3-}$ symmetric stretching vibrations. Bands at 936 and 843 cm^{-1} may be connected with δ M–OH bending vibrations or with librations modes of water molecules or hydroxyls. Bands at 613 and 485 cm^{-1} are assigned to the ν_4 (δ) $(PO_4)^{3-}$ and to the ν_2 (δ) $(PO_4)^{3-}$ bending vibrations, respectively. The basic characteristics of the experimental IR spectrum of tvrdýite correspond to published infrared spectra of isostructural beraunite (Chukanov, 2014; Frost *et al.,* 2014).

Tvrdýite was also investigated with a confocal Nicolet DXR Raman microscope. The Raman signal was excited by a 532 laser and detected with a multichannel air-cooled CCD camera. The laser power at the sample was limited to 1 mW to avoid possible thermal destruction of the samples. Spectra were recorded between 100 and 2000 cm^{-1} with a resolution of 4 cm^{-1} and a minimum lateral resolution of ~1 μm on the sample (Fig. 7). The main bands observed are (cm^{-1}) at 1623, 1194, 1102, 1023, 860, 698, 637, 586, 496, 415, 303, 281, 233 and 143. The broad band at 1623 cm^{-1} is related to the ν_2 (δ) bending vibrations of water molecules. Bands at 1194 and 1102 cm^{-1} are attributed to the ν_3 $(PO_4)^{3-}$ antisymmetric stretching vibrations, and that at 1023 cm^{-1} to the ν_1 $(PO_4)^{3-}$ symmetric stretching vibrations. A band at 860 cm^{-1} is related to the δM–OH bending vibrations or to the libration modes of water molecules or hydroxyls. The ν_4 (δ) $(PO_4)^{3-}$ bending vibrations are connected with the bands at 698, 637 and 586 cm^{-1}, and the ν_2 (δ) $(PO_4)^{3-}$ bending vibrations with the bands at 496 and 415 cm^{-1}. According to Frost *et al.* (2014), bands at 303 and 281 cm^{-1} may be related to the metal oxygen stretching vibrations, and those at 233 and 143 cm^{-1} may be described as external or lattice vibrations.

According to Pechkovskii *et al.* (1981), it may be concluded that only the presence of phosphate ions, $(PO_4)^{3-}$ in the structure of tvrdýite, may be inferred from the infrared and Raman spectra. This conclusion differs from that of the infrared and Raman spectra of isostructural beraunite taken from Frost *et al.* (2014), in which not only $(PO_4)^{3-}$, but also $(OHPO_3)^{2-}$ ions should be observed in the infrared and Raman spectra. However, splitting of doubly and triply degenerate $(PO_4)^{3-}$ and $(HOPO_3)^{2-}$ (or fragments PO_3 and POH)) stretching and bending vibrations and overlapping of related bands make any unambiguous assignment of $(HOPO_3)^{2-}$ groups in the presence of $(PO_4)^{3-}$ difficult.

Powder diffraction

Powder XRD data for tvrdýite were collected on a Bruker D8 Advance diffractometer (National

TABLE 2. Powder XRD data (d_{hkl} in Å) for tvrdýite.

I_{obs}	I_{calc}	$d_{obs.}$	d_{calc}	h	k	l
100.0	100.0	10.227	10.251	2	0	0
5.5	38.2	9.400	9.419	0	0	2
13.8	20.4	7.156	7.166	2	0	$\bar{2}$
1.0	4.6	6.716	6.726	2	0	2
7.0	5.9	5.120	5.125	4	0	0
1.0	18.8	4.769	4.770	1	1	1
0.7	3.6	4.707	4.710	0	0	4
0.5	1.0	4.383	4.387	2	0	$\bar{4}$
0.6	13.1	4.353	4.354	1	1	2
0.3	3.3	4.087	4.088	3	1	0
0.7	9.4	3.701	3.699	3	1	2
0.8	0.9	3.579	3.583	4	0	$\bar{4}$
11.4	9.4	3.416	3.417	6	0	0
0.5	6.1	3.364	3.368	3	1	3
5.6	3.2	3.278	3.280	6	0	$\bar{2}$
0.6	6.4	3.196	3.196	5	1	0
2.4	8.2	3.140	3.140	0	0	6
0.3	6.8	3.123	3.125	5	1	1
1.4	5.8	3.057	3.057	2	0	$\bar{6}$
2.3	32.7	3.031	3.031	3	1	4
1.3	1.1	2.853	2.853	6	0	$\bar{4}$
0.8	8.2	2.708	2.708	5	1	$\bar{4}$
0.3	7.4	2.670	2.670	1	1	$\bar{6}$
5.0	5.3	2.562	2.563	8	0	0
0.6	4.5	2.540	2.540	7	1	0
0.3	0.3	2.513	2.514	8	0	$\bar{2}$
0.8	0.6	2.3138	2.3136	8	0	$\bar{4}$
0.6	3.6	2.2890	2.2888	7	1	$\bar{4}$
0.7	1.4	2.1941	2.1933	4	0	$\bar{8}$
0.8	8.9	2.0757	2.0749	3	1	$\bar{8}$
3.1	3.7	2.0511	2.0501	10	0	0
0.5	5.3	1.9809	1.9819	6	2	2
0.3	2.4	1.9418	1.9423	5	1	$\bar{8}$
0.2	5.9	1.9020	1.9015	6	2	$\bar{4}$
0.2	2.3	1.8360	1.8351	3	1	9
0.3	0.3	1.7079	1.7084	12	0	0
0.3	2.1	1.6954	1.6959	6	0	$\overline{10}$
0.6	1.5	1.6632	1.6626	12	0	2
1.1	0.9	1.6405	1.6398	12	0	$\bar{4}$
0.5	7.7	1.5986	1.5979	10	2	0
0.4	0.7	1.4639	1.4644	14	0	0
0.8	1.4	1.4268	1.4266	12	0	$\bar{8}$

Museum, Prague) with a solid state 1D LynxEye detector using Cu$K\alpha$ radiation and operating at 40 kV and 40 mA. The powder pattern was collected using Bragg–Brentano geometry in the range 4–70°2θ, in 0.01° steps with a counting time of 30 s per step. Positions and intensities of diffractions were found and refined using the *PearsonVII* profile-shape function with the *ZDS* program package (Ondruš, 1993) and the unit-cell parameters were refined by the least-squares algorithm implemented by Burnham (1962). The experimental powder pattern was indexed in accordance with the calculated values of intensities obtained from the crystal structure refinement, based on the Lazy Pulverix program (Yvon *et al.*, 1977). The experimental powder data given in Table 2 agree with the pattern calculated from single-crystal data; experimental intensities are affected by preferred orientation caused by the good (100) cleavage and by the fibrous nature of studied mineral. The refined unit-cell parameters of tvrdýite are $a = 20.543(2)$, $b = 5.101(1)$, $c = 18.877(4)$ Å, $\beta = 93.64(1)^{o}$ and $V = 1974.1(6)$ Å^3.

Single-crystal X-ray diffraction

A needle-shaped crystal 0.005 mm in diameter and 0.07 mm long was separated carefully from the surface of a high-Al fibrous sheath for study at the microfocus macromolecular beamline MX2 of the Australian Synchrotron. Data were collected at 100 K using an ADSC Quantum 315r detector and monochromatic radiation with a wavelength of 0.71073 Å. A phi scan was employed with a frame width of 1° and a counting time per frame of 2 s. The image plate data were processed using *XDS* software to produce intensity data that were refined using *SHELXL* (Sheldrick, 2008). A total of 19,435 reflections was collected to a maximum $\theta = 30°$, giving 2744 unique reflections with $R_{int} = 0.057$. Details of data collection and refinement are given in Table 3.

A structure solution was obtained using *SHELXT* (Sheldrick, 2008), which confirmed the beraunite structure as reported by Moore and Kampf (1992), but with an origin shift of (½,0,½). The origin was relocated to conform to previous studies (Fanfani and Zanazzi, 1967; Marzoni Fecia di Cossato, *et al*., 1989; Moore and Kampf, 1992) and the structure was refined using *SHELXL* (Sheldrick, 2008). Site occupancy refinements were made with zinc substitution for iron at *M*1, for which the iron was confirmed to be predominantly Fe^{2+} by Moore and Kampf (1992). Aluminium substitution for trivalent iron was incorporated at the sites *M*2 through *M*4. Substitution of As for P in the *P*1 and *P*2 sites was also tested, but the site occupancy factor for As refined to zero. A difference-Fourier synthesis showed the positions of all nine expected H atoms based on previous studies. The O–H distances were restrained to be 0.95(2) Å and the

TABLE 3. Summary of data collection conditions and refinement parameters for tvrdýite.

Simplified formula	$Fe^{2+}Fe_2^{3+}Al_3(PO_4)_4(OH)_5(OH_2)_4 \cdot 2H_2O$
Temperature	100 K
Wavelength	0.71073 Å
Crystal system	Monoclinic
Space group	*C*2/*c*
Unit-cell dimensions	$a = 20.564(4)$ Å $b = 5.1010(10)$ Å $c = 18.883(4)$ Å $\beta = 93.68(3)°$
Volume	1976.7(7) Å^3
Z	4
Density (calculated)	2.76 g cm^{-3}
Absorption coefficient	3.009 mm^{-1}
Absorption correction	SADABS, $T_{min}/T_{max} = 0.707/0.746$
Crystal size (mm)	0.005 × 0.005 × 0.05
Theta range for data collection	2.16 to 30.01°.
Index ranges	$-28 \le h \le 28$, $-6 \le k \le 6$, $-26 \le l \le 26$
Reflections collected	19,435
Independent reflections	2744 [$R_{int} = 0.0571$]
Completeness to $\theta = 30.01°$	95.3%
Refinement method	Full-matrix least-squares on F^2
Data / restraints / parameters	2744 / 12 / 204
Goof on F^2	1.053
Final *R* indices [$I>2\sigma(I)$]	$R_1 = 0.0384$
R indices (all data)	$R_1 = 0.0506$, $wR_2 = 0.0958$
Extinction coefficient	0.0033(3)
Largest diff. peak and hole	0.73 and –0.62 e^- Å^{-3}

H–H distances for the water molecules were restrained to be 1.45(3) Å. An overall isotropic displacement parameter was refined for the H atoms, while all other atoms were refined with anisotropic displacement parameters. The final agreement factors are $R_1 = 0.038$ for 2276 observed reflections with $I > 2\sigma(I)$ and 0.051 for all reflections. Refined atom coordinates, equivalent isotropic displacement parameters and site occupancies are reported in Table 4. Polyhedral bond distances and valence sums for the metal atoms are given in Table 5. Hydrogen-bonding details are reported in Table 6.

Crystal structure of tvrdýite

The refined structure for tvrdýite is shown in projection along the *b* axis in Fig. 8. A key feature of the structure, as described in detail by Moore (1970), is the presence of linear face-shared octahedral trimers, called *h*-clusters by Moore (1970). These trimers, with *M*1 as the central atom and *M*4 as the terminal atom, are aligned along $[10\bar{1}]$ and are interconnected by corner sharing with pairs of *M*3 octahedra along [001] and with PO_4 tetrahedra along [010] to form dense slabs parallel to (100). The connection between the slabs is through corner-sharing of the terminal octahedra of the trimers with $M2O_2(OH)_2(OH_2)_2$ octahedra. This linkage creates an open framework structure with large 10-sided channels running parallel to [010], which are occupied by water molecules (O14 in Table 4). The structure also contains smaller channels with hexagonal cross-section running parallel to $[10\bar{1}]$, as shown in Fig. 9. This shows that the Al-dominant sites, *M*2 and *M*3, and the Fe-dominant sites, *M*1 and *M*4, form separate bands, which alternate parallel to (101).

Almost full ordering of Al occurs in the octahedra centred on *M*2 (92%Al + 8%Fe), while the *M*3 site is two thirds occupied by Al. The *M*1 and *M*4 octahedra of the face-sharing trimers contain predominately Fe. The bond-valence sum at site *M*1 is 2.46, indicating that this site contains approximately equal amounts of Fe^{3+} and Fe^{2+}.

TABLE 4. Atom coordinates (x 10^4) and equivalent isotropic displacement parameters (Å^2 × 10^3) for tvrdýite. U_{iso} is defined as one third of the trace of the orthogonalized U^{ij} tensor.

Atom	s.o.f.	*x*/*a*	*y*/*b*	*z*/*c*	U_{iso}
M(1)	0.92(2) Fe + 0.08(2) Zn	0	0	0	13(1)
M(2)	0.919(7) Al + 0.081(7) Fe	¼	¼	0	12(1)
M(3)	0.670(5) Al + 0.330(5) Fe	442(1)	2775(1)	1733(1)	12(1)
M(4)	0.680(6) Fe + 0.320(6) Al	1092(1)	371(1)	4154(1)	12(1)
P(1)		1062(1)	4727(1)	260(1)	11(1)
P(2)		4083(1)	429(2)	1814(1)	13(1)
O(1)		1797(1)	4758(5)	171(1)	18(1)
O(2)		4261(1)	2497(4)	204(1)	16(1)
O(3)		4219(1)	2396(5)	5004(1)	19(1)
O(4)		917(1)	4328(5)	1029(1)	21(1)
O(5)		4807(1)	465(5)	1659(1)	17(1)
O(6)		994(1)	4779(5)	2401(1)	22(1)
O(7)		3794(1)	3162(5)	1658(1)	20(1)
O(8)		1310(1)	3450(5)	3652(1)	17(1)
O(9)		65(1)	477(5)	3926(1)	20(1)
O(10)		1935(1)	143(4)	4645(1)	17(1)
O(11)		0	1211(6)	¼	17(1)
O(12)		3879(1)	4893(5)	3173(2)	29(1)
O(13)		2488(1)	972(5)	948(1)	18(1)
O(14)		2302(1)	3578(6)	2160(2)	26(1)
H(1)		0(30)	–1140(60)	3740(30)	71(7)
H(2)		1970(30)	1580(80)	4910(30)	71(7)
H(3)		0	–520(40)	¼	71(7)
H(4)		4050(30)	6480(60)	3090(30)	71(7)
H(5)		3850(30)	4070(110)	2754(19)	71(7)
H(6)		2840(20)	–10(100)	1050(30)	71(7)
H(7)		2420(30)	2110(100)	1300(20)	71(7)
H(8)		2530(20)	5060(70)	2260(40)	71(7)
H(9)		1876(11)	3970(110)	2190(4)	71(7)

s.o.f. = site occupancy factor

This was expected to be the site in which the Zn was incorporated, but the site refinement gave only 8% Zn in *M*1, which corresponds to ~20% of the amount of Zn measured by EPMA. A consideration of bond valences in Table 5 suggests that the most likely sites for the majority of the zinc are the terminal octahedra of the face-sharing trimers, *M*4. This was checked by a refinement in which a fixed amount of Zn was included in *M*4 and the Al and Fe occupancies refined. The result was inconclusive, with no improvement in the *R* factor and with an increase in the Al/Fe ratio in *M*4 that was not consistent with the EPMA results.

The H-bonding scheme is reported in Table 6. The bonds involve O−O distances in the range 2.69 to 3.34 Å, which correspond to medium to weak bonds. The stronger of the bonds are associated with the coordinated H_2O molecules bonded to *M*2 (O13) and *M*3 (O12) as donors. The acceptors are the channel water molecules (O14) and phosphate oxygen (O6), respectively.

Electron probe microanalyses show strong element-element correlations for Al-Fe (negative) and for Al-F (positive). The latter is consistent with Al replacement for Fe in beraunite being due to reaction with F-rich acidic solutions. The average amount of F is only ~0.2 F pfu. It could not be located in the structure analysis, but would be expected to substitute at the hydroxyl sites O10 and O11 coordinated to the Al-dominant sites *M*2 and *M*3, respectively. The EPMA data show only weak correlation between As and P, consistent with the structure analysis, and suggests that As may be fully disordered at the tetrahedral sites.

TABLE 5. Polyhedral bond lengths (Å) and cation valence sums (valence units) for tvrdýite.

M(1)–O(2) x2	2.040(2)	M(2)–O(10) x2	1.875(2)
M(1)–O(9) x2	2.055(2)	M(2)–O(1) x2	1.893(2)
M(1)–O(3) x2	2.084(2)	M(2)–O(13) x2	1.954(2)
Average	2.060		1.907
Valence sum	2.46		3.09
M(3)–O(4)	1.875(3)	M(4)–O(8)	1.903(2)
M(3)–O(5)	1.893(2)	M(4)–O(10)	1.917(2)
M(3)–O(11)	1.931(2)	M(4)–O(7)	1.928(3)
M(3)–O(6)	1.934(3)	M(4)–O(2)	2.064(2)
M(3)–O(9)	1.961(2)	M(4)–O(3)	2.090(2)
M(3)–O(12)	2.027(3)	M(4)–O(9)	2.128(2)
Average	1.937		2.005
Valence sum	3.11		2.92
P(1)–O(4)	1.514(3)	P(2)–O(8)	1.535(2)
P(1)–O(1)	1.531(2)	P(2)–O(7)	1.536(3)
P(1)–O(3)	1.549(2)	P(2)–O(6)	1.537(3)
P(1)–O(2)	1.557(2)	P(2)–O(5)	1.537(2)
Average	1.538		1.536
Valence sum	4.96		4.98

Tvrdýite is isostructural with the basic iron phosphate mineral beraunite, $Fe^{2+}Fe^{3+}_5(PO_4)_4(OH)_5(OH_2)_4{\cdot}2H_2O$ (Fanfani and Zanazzi, 1967; Marzoni Fecia di Cossato, *et al*., 1989; Moore and Kampf, 1992). The most important difference is in the crystal chemistry, with two of the four independent *M* sites containing dominant Al in tvrdýite. Comparative data for the two minerals are given in Table 7. The replacement of the majority of Fe by Al in the *M*2 and *M*3 sites results in a relatively large unit-cell volume decrease of 5.1%, with the largest decrease associated with the *c* axis (2.0% decrease).

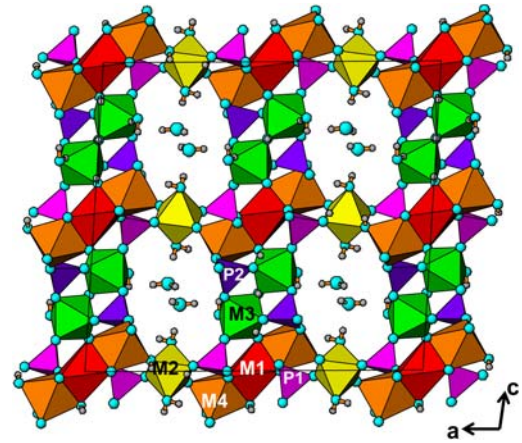

FIG. 8. Projection along [010] of the structure for tvrdýite. Metal atoms are labelled. H atoms are small grey spheres.

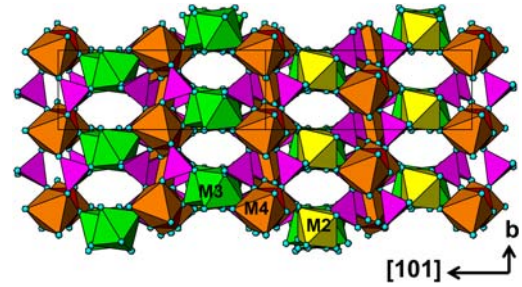

FIG. 9. View of the structure of tvrdýite along [10$\bar{1}$].

Acknowledgements

The constructive comments of Associate Editor Juro Majzlan, Structure Editor Peter Leverett and the reviewers helped to improve the quality of the earlier

TABLE 6. Hydrogen bonding in tvrdýite (Å, °).

D–H···A	d(D–H)	d(H···A)	d(D···A)	<(DHA)
O(9)–H(1)···O(5)	0.90(2)	1.94(3)	2.804(3)	159(6)
O(10)–H(2)···O(1)	0.89(2)	1.97(3)	2.806(3)	156(6)
O(11)–H(3)···O(5)	0.88(2)	2.608(16)	3.345(4)	141.8(3)
O(12)–H(4)···O(6)	0.90(2)	1.92(4)	2.737(4)	150(6)
O(12)–H(5)···O(7)	0.895(19)	2.12(3)	2.989(4)	164(5)
O(13)–H(6)···O(8)	0.899(19)	1.96(2)	2.845(3)	169(6)
O(13)–H(7)···O(14)	0.893(19)	1.83(3)	2.695(4)	164(6)
O(14)–H(8)···O(14)	0.899(19)	2.12(4)	2.946(3)	152(6)
O(14)–H(9)···O(6)	0.90(2)	1.92(2)	2.824(3)	172(6)

TABLE 7. Comparative data for tvrdýite and beraunite (Moore and Kampf, 1992).

	Tvrdýite	Beraunite
Formula	$Fe^{2+}Fe_2^{3+}Al_3(PO_4)_4(OH)_5(OH_2)_4{\cdot}2H_2O$	$Fe^{2+}Fe_5^{3+}(PO_4)_4(OH)_5(OH_2)_4{\cdot}2H_2O$
Symmetry	Monoclinic, *C2/c*	Monoclinic, *C2/c*
Cell	$a = 20.564(4)$, $b = 5.101(1)$, $c = 18.883(4)$ Å, $\beta = 93.68(3)°$ $V = 1976.7$ Å^3	$a = 20.953(5)$, $b = 5.171(1)$, $c = 19.266(4)$ Å, $\beta = 93.34(2)°$ $V = 2083.9$ Å^3
Z	4	4
Strongest powder pattern lines *d, I, hkl*	10.227, 100 (200) 7.156, 14 (20$\bar{2}$) 3.416, 11 (600) 5.120, 7 (400) 3.278, 6 (60$\bar{2}$) 9.400, 6 (002)	10.37, 100 (200) 4.825, 60 (111) 3.082, 60 (314) 9.58, 50 (002) 7.229, 50 ($\bar{2}$02) 4.418, 50 (112)
Optics	Biaxial (–) $\alpha = 1.650$, $\beta = 1.671$, $\gamma = 1.677$	Biaxial (+) $\alpha = 1.775$, $\beta = 1.786$, $\gamma = 1.815$

version of the manuscript. We thank Radek Škoda (Masaryk University, Brno) and Ján Pásztor (Nicolet, Prague) for their kind assistance with the collection of the EPMA and spectroscopy data. This work was supported financially by project NAKI-DF12P01OVV021 of the Ministry of Culture of the Czech Republic for JS and DKRVO 2016/02 (00023272) to JČ. Further support was from the John Jago Trelawney Endowment to the Mineral Sciences Department of the Natural History Museum of Los Angeles County for ARK.

References

Anthony, J.W., Bideaux, R.A., Bladh, K.W. and Nichols, M.C. (2000) *Handbook of Mineralogy, volume IV, Arsenates, Phosphates, Vanadates.* Mineral Data Publishing, Tucson, Arizona.

Beran, P. and Sejkora, J. (2006) The Krásno Sn-W ore district near Horní Slavkov: mining history, geological and mineralogical characteristics. *Journal of the Czech Geological Society*, **51**, 3–42.

Breithaupt, A. (1841) *Vollständiges Handbuch der Mineralogie.* Arnoldische Buchhandlung, Dresden und Leipzig, Volume **2**, p. 156.

Burnham, C.W. (1962) Lattice constant refinement. *Carnegie Institute Washington Yearbook*, **6**, 132–135.

Chukanov, N.V. (2014) *Infrared Spectra of Minerals, Extended Library.* Springer, Dodrecht, The Netherlands.

Fanfani, L. and Zanazzi, P.F. (1967) The crystal structure of beraunite. *Acta Crystallographica*, **22**, 173–181.

Frost, R.L., López, A., Scholz, R., Xi, Y. and Lana, C. (2014) The molecular structure of the phosphate mineral beraunite $Fe^{2+}Fe_5^{3+}(PO_4)_4(OH)_5.4H_2O$. *Spectrochimica Acta Part A: Molecular and Biomolecular Spectroscopy*, **128**, 408–412.

Gunter, M.E., Bandli, B.R., Bloss, F.D., Evans, S.H., Su, S.C. and Weaver, R. (2004) Results from a McCrone spindle stage short course, a new version of EXCALIBR, and how to build a spindle stage. *The Microscope*, **52**, 23–39.

Libowitzky, E. (1999) Correlation of O-H stretching frequencies and OH···O hydrogen bond lengths in minerals. *Monatshefte für Chemie*, **130**, 1047–1059.

Lutz, H.D. (1995) Hydroxide ions in condensed materials – Correlation of spectroscopic and structural data. *Structure and Bonding*, **82**, 86–103.

Mandarino, J.A. (1981) The Gladstone-Dale relationship: Part IV. The compatibility concept and its application. *The Canadian Mineralogist*, **19**, 441–450.

Marzoni Fecia di Cossato, Y., Orlandi, P. and Pasero, M. (1989) Manganese-bearing beraunite from Mangualde, Portugal: mineral data and structure refinement. *The Canadian Mineralogist*, **27**, 441–446.

Mills, S.J., Kolitsch, U., Birch, W.D. and Sejkora, J. (2008) Kunatite, $CuFe_2^{3+}(PO_4)_2(OH)_2{\cdot}4H_2O$, a new member of the whitmoreite group, from Lake Boga, Victoria, Australia. *Australian Journal of Mineralogy*, **14**, 3–12.

Mills, S.J., Kampf, A.R., Sejkora, J., Adams, P.M., Birch, W.D. and Plášil, J. (2011) Iangreyite: a new secondary phosphate mineral closely related to perhamite. *Mineralogical Magazine*, **75**, 327–336.

Mills, S.J., Sejkora, J., Kampf, A.R., Grey, I.E., Bastow, T. J., Ball, N.A., Adams, P.M., Raudsepp, M. and Cooper, M.A. (2012) Krásnoite, the fluorophosphate analogue of perhamite, from the Huber open pit, Czech Republic and the Silver Coin mine, Nevada, USA. *Mineralogical Magazine*, **76**, 625–634.

Moore, P.B. (1970) Crystal chemistry of the basic iron phosphates. *American Mineralogist*, **55**, 135–169.

Moore, P.B. and Kampf, A.R. (1992) Beraunite: refinement, comparative crystal chemistry, and selected bond valences. *Zeitschrift fur Kristallographie*, **201**, 263–281.

Nakamoto, K. (1986) *Infrared and Raman spectra of Inorganic and Coordination Compounds.* John Wiley and Sons, New York.

Ondruš, P. (1993) A computer program for analysis of X-ray powder diffraction patterns. *Materials Science Forum, EPDIC-2, Enchede*, **133–136**, 297–300.

Pažout, R., Sejkora, J., Maixner, J., Dušek, M. and Tvrdý, J. (2015) Refikite from Krásno, Czech Republic: a crystal and molecular-structure study. *Mineralogical Magazine*, **79**, 59–70.

Pechkovskii, V.V., Mel'nikova, R.Ya., Dzyuba, E.D., Barannikova, T.I., Nikanovich, M.V. (1981) *Atlas of Infrared Spectra of Phosphates. Orthophosphates.* Nauka, Moscow.

Plášil, J. and Tvrdý, J. (2008) Uranopilite and jáchymovite from uranium deposit Horní Slavkov. *Bulletin mineralogicko-petrologického oddělení Národního muzea v Praze*, **16**, 61–64.

Pouchou, J.L. and Pichoir, F. (1985) "PAP" (φ ρZ) procedure for improved quantitative microanalysis. Pp. 104–106 in: *Microbeam Analysis* (J.T. Armstrong, editor). San Francisco Press, San Francisco, USA.

Sejkora, J. and Tvrdý, J. (2009) Seltene und neue Mineralien aus den Zinnlagerstätten des Erzreviers Horní Slavkov. *Lapis*, **34**, 53–62.

Sejkora, J., Ondruš, P., Fikar, M., Veselovský F., Mach, Z., Gabašová, A., Škoda, R. and Beran, P. (2006*a*) Supergene minerals at the Huber stock and Schnöd stock deposits, Krásno ore district, the Slavkovský les area, Czech Republic. *Journal of the Czech Geological Society*, **51**, 57–101.

Sejkora, J., Škoda, R. and Ondruš, P. (2006*b*) New naturally occurring mineral phases from the Krásno – Horní Slavkov area, western Bohemia, Czech Republic. *Journal of the Czech Geological Society*, **51**, 159–187.

Sejkora, J, Škoda, R., Ondruš, P., Beran, P. and Süsser, C. (2006*c*) Mineralogy of phosphate accumulations in the Huber stock, Krásno ore district, Slavkovský les area, Czech Republic. *Journal of the Czech Geological Society*, **51**, 103–147.

Sejkora, J., Bureš, B. and Tvrdý, J. (2008) Nordstrandit von Depoltovice bei Karlovy Vary (Karlsbad), Tschechien. *Lapis*, **33**, 36–38.

Sejkora, J., Plášil, J. and Filip, J. (2011) Plimerite from Krásno near Horní Slavkov ore district, Czech Republic. *Journal of Geosciences*, **56**, 215–229.

Sheldrick, G.M. (2008) A short history of SHELX. *Acta Crystallographica, A64*, 112–122.

Tvrdý, J. and Plášil, J. (2010) Jáchymov – Reiche Erzlagerstätte und Radonbad im böhmischen Westerzgebirge. *Aufschluss*, **61**, 277–292.

Yvon, K., Jeitschko, W. and Parthé, E. (1977) Lazy Pulverix, a computer program for calculation X-ray and neutron diffraction powder patterns. *Journal of Applied Crystallography*, **10**, 73–74.